Journal of Power Sources 225 (2013) 13–19

Contents lists available at SciVerse ScienceDirect

Journal of Power Sources

journal homepage: www.elsevier.com/locate/jpowsour

Stabilization of cubic lithium-stuffed garnets of the type "$Li_7La_3Zr_2O_{12}$" by addition of gallium

Hany El Shinawi*,[1], Jürgen Janek

Physikalisch-Chemisches Institut, Justus Liebig Universität Giessen, Heinrich-Buff-Ring 58, 35392 Giessen, Germany

HIGHLIGHTS

- ► $Li_7La_3Zr_2O_{12}$ garnets, with cubic structure and fast lithium ion conductivity were stabilized by gallium addition.
- ► Materials with good sinterability, at low sintering time and temperature, were obtained.
- ► The new approach provides a quantitative and reproducible route of synthesis.
- ► Gallium addition stabilizes the cubic garnet phase at gallium content ≥0.3 moles per mole of $Li_7La_3Zr_2O_{12}$.
- ► Excess gallium, in the form of $LiGaO_2$, resided at grain boundaries and acts as a sintering aid, which improves conductivity.

ARTICLE INFO

Article history:
Received 30 May 2012
Received in revised form
18 July 2012
Accepted 30 September 2012
Available online 11 October 2012

Keywords:
Gallium-modified $Li_7La_3Zr_2O_{12}$
Lithium-stuffed garnet
Fast lithium ion conductor
Lithium ion battery

ABSTRACT

Cubic lithium-stuffed garnets of the type $Li_7La_3Zr_2O_{12}$ have been successfully stabilized by incorporation of gallium. The materials have been prepared by a sol-gel procedure with final calcination at 1085 °C for 6 h. Under the applied synthesis conditions, 0.3 mole of gallium ions (per mole of $Li_7La_3Zr_2O_{12}$) were sufficient to fully stabilize the cubic garnet-type phase. Increasing the fraction of gallium led to significant improvement of sinterability and lithium ion conductivity. Excess gallium ions, in the form of $LiGaO_2$, act as a sintering aid and reside exclusively at the grain boundaries. The gallium-modified garnets showed conductivities up to 5.4×10^{-4} S cm^{-1} at 20 °C, and activation energies in the range 0.32–0.37 eV.

1. Introduction

An increasing interest is being directed to solid lithium electrolytes as promising candidates for a next generation of environmentally benign and technologically outstanding lithium ion batteries. Among crystalline solid electrolytes, lithium-containing garnets have attracted recent interest due to their high lithium ion conductivity. Among several garnet phases being investigated, the lithium–lanthanum–zirconium garnet (LLZO) shows the most promising properties, as it combines the high ionic conductivity with minor electronic conductivity and good stability in contact with metallic lithium [1,2]. In a first report, Murugan et al. described the synthesis of the LLZO phase by solid-state reaction at 1230 °C [1]. This high-temperature synthesized LLZO phase (HT-LLZO) showed cubic symmetry and excellent transport and electrochemical properties. The high-temperature synthesis proved to be vital for obtaining well-sintered material, and the resulting cubic symmetry is essential for high lithium ion mobility. Tetragonal LLZO [3–5] as well as low-temperature synthesized LLZO (LT-LLZO) phases [5,6] have also been prepared. In contrast, tetragonal LLZO phases show poor lithium ion conductivity, and the sinterability of the LT-LLZO phases appears to be insufficient for conducting conductivity tests and applications.

The stoichiometric composition $Li_7La_3Zr_2O_{12}$ was proposed for the cubic HT-LLZO phase synthesized by Murugan et al. [1]. This stoichiometry, $Li_7La_3Zr_2O_{12}$, has also been suggested for tetragonal LLZO and cubic LT-LLZO phases through neutron diffraction studies [3,6]. However, recent studies on cubic HT-LLZO phases strongly indicate that the stoichiometry of these fast ion-conducting phases is altered either by vacancy formation and/or inclusion of foreign ions [4,7–9]. Experimental studies, indeed, indicate that the formation of the cubic HT-LLZO is generally associated with incorporation of foreign ions such as aluminium ions [4,7–12].

* Corresponding author. Tel.: +49 641 99 34514/34501; fax: +49 641 99 34509.
E-mail addresses: hany.el-shinawi@phys.chemie.uni-giessen.de (H. El Shinawi), juergen.janek@phys.chemie.uni-giessen.de (J. Janek).
[1] Permanent address: Chemistry Department, Faculty of Science, Mansoura University, 35516 Mansoura, Egypt.

0378-7753/$ – see front matter © 2012 Elsevier B.V. All rights reserved.
http://dx.doi.org/10.1016/j.jpowsour.2012.09.111

Significant amounts of aluminium were detected in different HT-LLZO phases, and are thought to be diffused from alumina crucibles into LLZO samples during high-temperature sintering step [7–9]. The addition of aluminium has also been tested in an attempt to investigate its role in stabilization of the cubic LLZO phases [8–11]. It has been suggested that the Al^{3+} ions reside at the grain boundaries where an amorphous Li_2O–Al_2O_3 phase supports sintering and leads to the blocking of Li loss at higher temperatures. Amorphous Li–Al–Si–O/$LiAlSiO_4$ was observed at the grain boundaries of Al/Si-doped LLZO phases [9]. The effect of Al^{3+} ions as sintering aid, however, seems not to be the main effect of these ions in order to stabilize the cubic HT-LLZO phases. Diffusion of these ions inside the LLZO grains is also detected [7,8]. Studies also suggest possible substitution of Al^{3+} ions for Li^+ ions in such a way that Li^+ ion vacancies are created and Li^+ ions are redistributed in the garnet structure. Neutron diffraction studies on cubic LT-LLZO and tetragonal LLZO phases suggest that the symmetry adapted by the LLZO phase (cubic or tetragonal) is highly connected to the distribution of lithium ions between tetrahedral and interstitial sites [3,6].

Recently, aluminium incorporation into LLZO, which is the current key for stabilization of cubic HT-LLZO phases, is being subjected to detailed quantitative studies [8,11]. We present in this report, however, a new approach to prepare cubic HT-LLZO phases in a quantitative and reproducible form. The cubic HT-LLZO phases were stabilized by addition of gallium, in the absence of aluminium, showing comparable structural and transport properties. Using the provided synthetic route, fast lithium ion-conducting phases are obtained at reduced calcination time and temperature.

2. Experimental

A sol-gel approach has been used to prepare the gallium-modified LLZO garnet phases. LLZO phases containing 0.0, 0.1, 0.2, 0.3, 0.4, 0.5 and 1.0 mole Ga per one mole of $Li_{7.8}La_3Zr_2O_{12+\delta}$ (referred to as 0.0Ga-LLZO, 0.1Ga-LLZO, 0.2Ga-LLZO, 0.3Ga-LLZO, 0.4Ga-LLZO, 0.5Ga-LLZO and 1.0Ga-LLZO, respectively) were synthesized. The excess lithium in $Li_{7.8}La_3Zr_2O_{12+\delta}$ was used to compensate for lithium loss during synthesis. Lithium acetate (Aldrich, 99.95%), lanthanum oxide (ChemPur, 99.99%), zirconium oxynitrate hydrate (Aldrich, 99%) and gallium acetylacetonate (Aldrich, 99.99%) were used as starting materials. Lanthanum oxide was preheated at 900 °C for 12 h before use; the degree of hydration in zirconium oxynitrate was determined experimentally by thermogravimetric analysis.

Stoichiometric amounts of the starting materials were first dissolved in hot dilute nitric acid. After cooling, EDTA (dissolved in NH_3 solution) was added to the mixture and followed by the addition of solid citric acid under stirring (mole ratio of total metal ions to EDTA and to citrate = 1:1:2). NH_4OH was then used to adjust the pH value of the solution to a value >7. Water was then evaporated at ~120 °C to produce a transparent yellowish brown gel. The gel was then heated at 250 °C to convert it to a black solid precursor. Then the solidified precursor was burnt in an electrical oven at 550 °C for 18 h to remove organic residues. The obtained powder was then isostatically pressed into pellets and calcined in air at 1085 °C for 6 h. An alumina disc covered with a thick platinum sheet was used as a sample holder for the calcination step. The sintered pellets were then either crushed to be examined by X-ray powder diffraction (XRD) or directly used for conductivity measurements.

XRD data were collected with an X'Pert Pro PANalytical diffractometer in reflection mode, using CuKα radiations. Rietveld refinements based on XRD data were performed using the GSAS suite of programs [13]. Scanning electron microscopy (SEM) and energy dispersive X-ray (EDX) studies were performed using a quantum MERLIN and X-Max (Oxford Instruments) machines, respectively.

AC impedance measurements were recorded using a potentiostat/galvanostat (model SP-300 from Biologic Science Instruments) in the frequency range of 7 MHz to 1 Hz and using an electrical perturbation of 20 mV. The data obtained were then analysed by the software package EC-Lab V10.02. Pellets with thickness 4–6 mm and diameter 10–13 mm were used in the conductivity measurements. Lithium (lithium foil, Chemetall) is used as electrode material, where lithium foil was pressed on the sides of the pellets and annealed at 140 °C for few minutes in order to improve adhesion. Copper or nickel wires were used to collect the current. The cells were then sealed in gas-tight pouches of aluminized compound foil. Sample preparation for conductivity measurements was exclusively performed under inert atmosphere in a glove box. Variable temperature conductivity measurements were carried out in a temperature chamber (WTL 64 Weiss Technik) in the temperature range 20–90 °C. Prior to each impedance measurement, the samples were equilibrated for 1 h at constant temperature. A slight increase in conductivity was observed by ageing. This effect may be linked to interfacial effects due to presence of $LiGaO_2$ at grain boundaries (see next section).

3. Results and discussion

3.1. Synthesis, structure and morphology

In an attempt to achieve a definite and reproducible synthetic route of gallium-modified LLZO phases, we decided to avoid using alumina crucibles and to minimize the contact between the sample and sample holder during the calcination step. After burning the gel at 550 °C, as described in Section 2, the isostatically pressed powder in the form of a pellet is sandwiched between two other thin pellets of the mother powder, and placed on an alumina disc covered with a thick platinum sheet. No contact between the main pellet and platinum or alumina was detected. For a given gallium content, different calcination temperatures and times were tested, showing a significant effect on the obtained products. After several experiments, we decided for sintering at "1085 °C for 6 h" as the best conditions, and then the effect of varying the gallium content was studied. After calcination step, the obtained pellets were either crushed to be examined by XRD or directly used for conductivity measurements.

XRD patterns collected from 0.0Ga-LLZO, 0.1Ga-LLZO, 0.2Ga-LLZO and 0.3Ga-LLZO samples are shown in Fig. 1. It can be seen that, under the applied synthesis conditions, the pure LLZO phase (0.0Ga-LLZO) has a predominant tetragonal symmetry (Fig. 1(a)). This is consistent with previous results reported for Al-free LLZO [8] and LLZO phases prepared by the sol-gel method [4,6]. On addition of gallium, the diffraction patterns changed gradually to represent phases with cubic symmetry. The sample containing 0.1 mole gallium (0.1Ga-LLZO) is typically a mixture of cubic and tetragonal phases (Fig. 1(b)). The 0.2Ga-LLZO sample contains mainly the cubic phase; however, a small reflection ($2\theta = 28.7^\circ$), corresponding to $La_2Zr_2O_7$ as an impurity, can be observed in the diffraction pattern (Fig. 1(c)). XRD, however, shows the 0.3Ga-LLZO sample as a single phase with cubic symmetry (Fig. 1(d)). The XRD pattern of the 0.3Ga-LLZO sample was readily indexed on a body-centred cubic unit cell, consistent with a garnet structure. Rietveld profile refinement based on the XRD data (see Supporting information, Fig. S1) confirmed the structure ($Ia\bar{3}\,d$ space group). No information about the occupancies of lithium ion sites could be extracted from the refinement. The refined cell constant a is 12.98279(5) Å, which is slightly larger than that previously reported for cubic LLZO

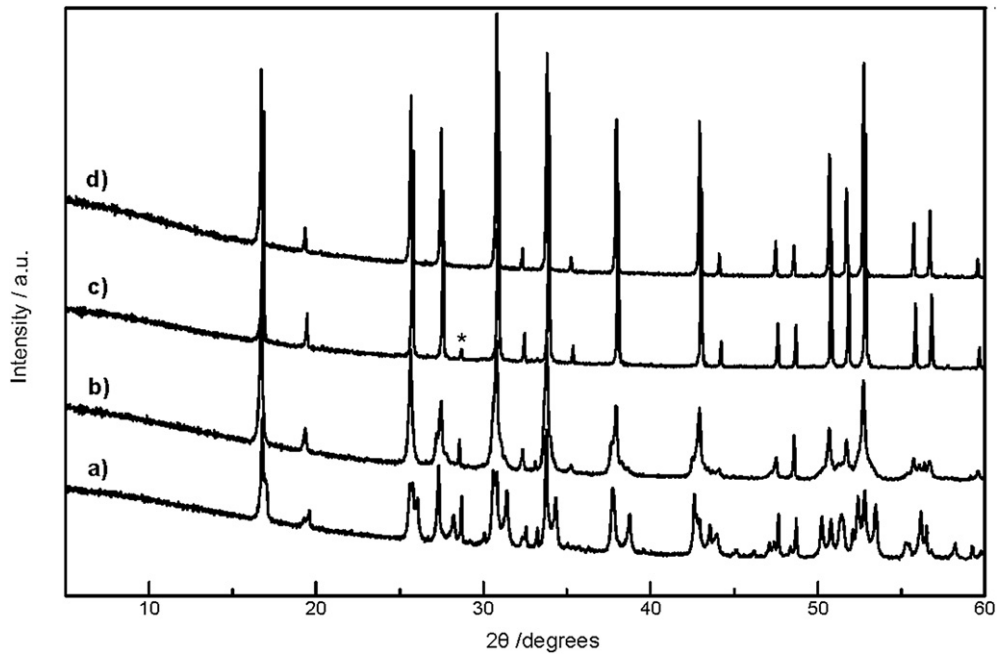

Fig. 1. XRD patterns of (a) 0.0Ga-LLZO, (b) 0.1Ga-LLZO, (c) 0.2Ga-LLZO and (d) 0.3Ga-LLZO samples. $K\alpha_2$ contribution was eliminated, using Rachinger method, for clarification. (*): $La_2Zr_2O_7$ (ICSD, PDF-01-075-0346).

phases [1,7,8]; the lattice constant reported by Murugan *et al.* is $a = 12.9682(6)$ Å. If gallium is accommodated in the garnet lattice, a bigger unit cell is in fact expected since the ionic radius of Ga is bigger than that of Al.

The investigation of the 0.3Ga-LLZO sample by SEM (Fig. 2(a)) indicates that the sample was insufficiently sintered. Attempts to improve sinterability by increasing the calcination temperature or the calcination time were unsuccessful. Increasing the calcination temperature, to higher than 1100 °C (for 6 h), led to the appearance of small reflections of $La_2Zr_2O_7$ impurity in the diffraction pattern. Extending calcination time (*e.g.* for 48 h), at the same calcination temperature (1085 °C), also gave rise to the same result. An attempt to improve sinterability by increasing the gallium content was therefore tested. Fig. 3 shows the XRD patterns of 0.4Ga-LLZO, 0.5Ga-LLZO and 1.0Ga-LLZO samples. It can be clearly seen that a cubic single phase is essentially retained for the 0.4Ga-LLZO sample (Fig. 3(a)). But impurity reflections were observed in the XRD patterns of 0.5Ga-LLZO and 1.0Ga-LLZO samples (Fig. 3(b,c)). It is also obvious that the amount of impurity phase(s) is higher for the 1.0Ga-LLZO sample. The major impurity phase was recognized as $LiGaO_2$, with traces of Li_2ZrO_3 as a second impurity. Nevertheless, SEM images of these samples (see Fig. 2(a–d)) indicate that the sinterability of the pellets was significantly enhanced by increasing gallium content. Excess gallium ions therefore combined with excess lithium ions, initially present in the samples, to form $LiGaO_2$ which served as a sintering agent. It can also be noted that no significant phase decomposition is observed as the gallium content is increased.

Fig. 2(e, f) shows cross-sectional SEM images of 0.3Ga-LLZO and 1.0Ga-LLZO samples, for comparison. It is clearly visible that the sample with excess gallium has smaller grain sizes and better densification. A closer inspection of the microstructure of this material shows a glass-like phase effectively spreading between the grains (Fig. 4(a)). EDX study of the system is shown in Fig. 4(b–d). EDX mapping reveals a predominant accumulation of gallium at the grain boundaries (Fig. 4(d)). Since $LiGaO_2$ has been detected as a major secondary phase in this material by XRD, it is suggested that $LiGaO_2$ is the main constituent of the intergranular phase. Small amounts of impurity phases containing zirconium and/or lanthanum may also contribute to this phase. This may account for the presence of traces of lanthanum and zirconium at the grain boundaries (Fig. 4(b, c)). Traces of Li_2ZrO_3, for example, have been detected in 1.0Ga-LLZO by XRD (Fig. 3(c)). Careful investigation of the gallium distribution pattern (Fig. 4(d)) shows a very faint distribution of gallium inside the grains; this may correspond to inclusion of gallium ions in the garnet lattice in order to support the formation of the cubic phase. However, further studies are required to confirm this suggestion. It is worth noting that XRD data collected from different Ga-containing materials show a slight lattice expansion in these materials compared with Al-containing materials. This would indicate the inclusion of Ga in the garnet lattice. However, no simple correlation between lattice volume and gallium content could be identified in the XRD patterns. Attempts to improve structural refinements by substituting Ga for Li and/or Zr in their crystal sites were also unsuccessful. Thus XRD data give no clear evidence of Ga inclusion in the garnet lattice. Neutron diffraction experiments are planned to get more information about the crystal structure of these materials.

3.2. Lithium ion conductivity

The conductivity of the successfully prepared cubic Ga-LLZO phases, namely 0.3Ga-LLZO, 0.4Ga-LLZO, 0.5Ga-LLZOand 1.0Ga-LLZO phases, was examined by AC impedance spectroscopy using Li metal electrodes. The impedance behaviour of the different materials was quite similar. Two semicircles were generally observed in the Nyquist plot. Over the studied frequency range, a shift of the observation window from left to right, *i.e.* towards lower frequencies, was detected as the gallium content increased. Fig. 5 shows typical impedance plots for 0.4Ga-LLZO, 0.5Ga-LLZO and 1.0Ga-LLZO samples at room temperature. The plots were generally fitted using (RQ)(RQ) equivalent circuits, except for the 1.0Ga-LLZO sample where plots were fitted using (R)(RQ) equivalent circuits in order to determine intercepts with the real Z axis.

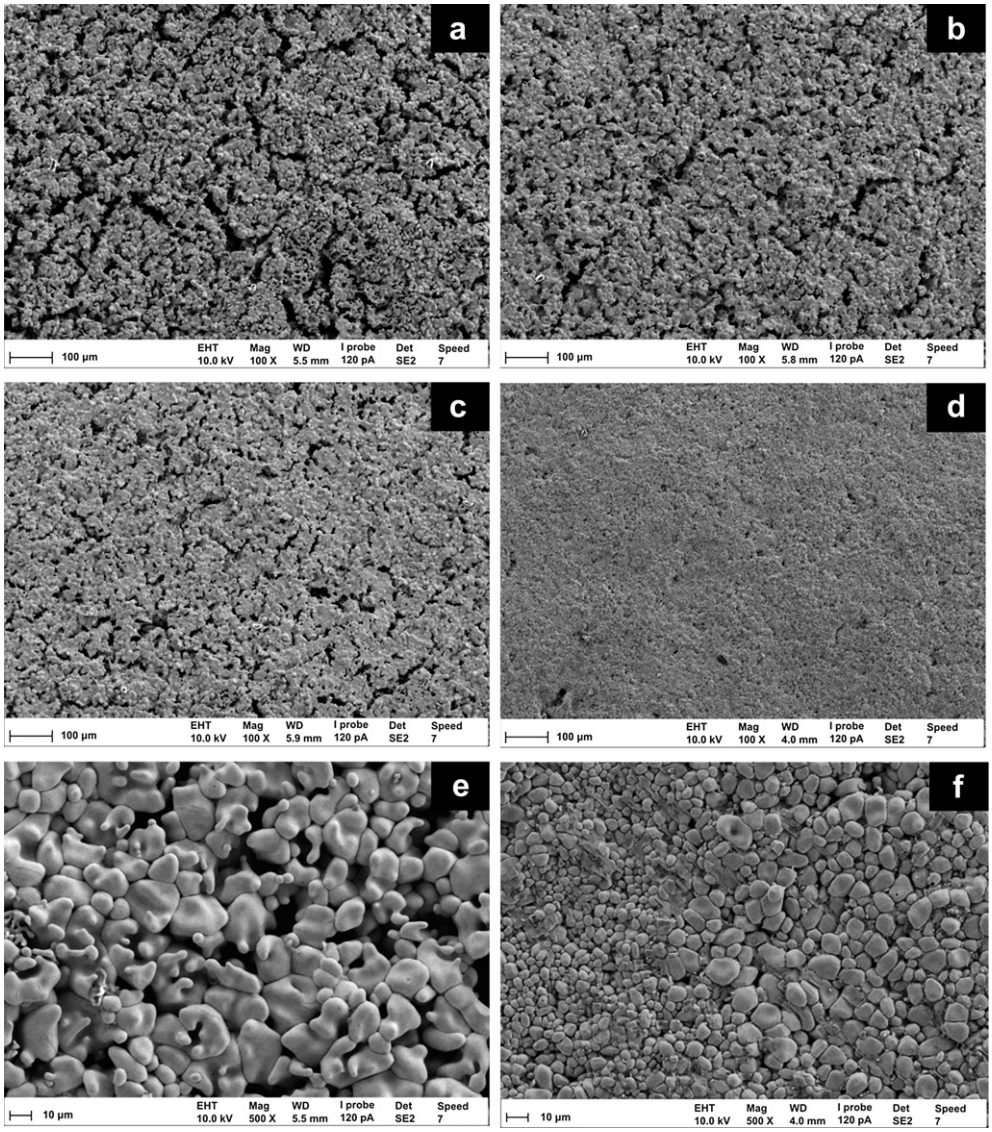

Fig. 2. Typical SEM images of (a) 0.3Ga-LLZO, (b) 0.4Ga-LLZO, (c) 0.5Ga-LLZO and (d) 1.0Ga-LLZO pellets. (e) and (f) show cross-sectional SEM images of 0.3Ga-LLZO and 1.0Ga-LLZO samples, respectively.

The electrode/electrolyte interface in the system Li/Li-electrolyte/Li is suggested to behave like a parallel resistance–capacitance circuit (RC), or RQ, described by a semicircle in the Z plane, which is assigned to the charge transfer at the interface [8,14,15]. Hence, the observation of the low frequency intercept with the real Z axis in different samples suggests, in general, that the observed transport effect is mainly ionic and corresponds to lithium ion mobility. The observation of two semicircles may then be interpreted in terms of bulk and grain-boundary effects (for the high frequency semicircle) and the electrode effects (for the low frequency semicircle). A second possibility is that the second semicircle observed at lower frequencies may represent grain-boundary or grain-boundary/electrode effects. The former approach is supported by detailed studies carried out in our group [8], and is also adopted elsewhere [9].

It might be useful here to consider the impedance behaviour of garnet-type electrolytes using Au blocking electrodes. Typical impedance plots of these materials using Au electrodes usually show two semicircles and a low frequency tail which are assigned to bulk, grain-boundary and electrode contributions, respectively [1,16–18]. However, spectra with unresolved contributions are also reported [2,17–19]; for the calculation of electrical conductivity in these cases, the intercept to the real axis was often taken as the total resistance. In order to validate an approach for calculating the conductivity of our samples, a comparison to this model was carried out. Two impedance measurements were therefore performed for the same 1.0Ga-LLZO sample using either Li electrodes or Au electrodes, respectively. The 1.0Ga-LLZO sample was chosen because it had good sinterability with respect to other samples. Au electrodes were gas-phase deposited on the circular sides of the pellet by thermal evaporation. The Nyquist plots of the two measurements are shown in Fig. 6; the inset shows a zoom in order to make the plot corresponding to Li electrodes visible. The measurement with the Au electrodes shows an unresolved small effect followed by a tail. This effect is indeed observed for cubic LLZO phases prepared by Kotobuki et al. [2] and is in consistence with the behaviour of other garnet-type Li ion-conducting phases. It can also be noted that, the intercept of the tail (in case of using Au electrodes) to the real Z axis approximately coincides with the intercept of the high frequency side of the observed semicircle (in case of using Li electrodes) on the

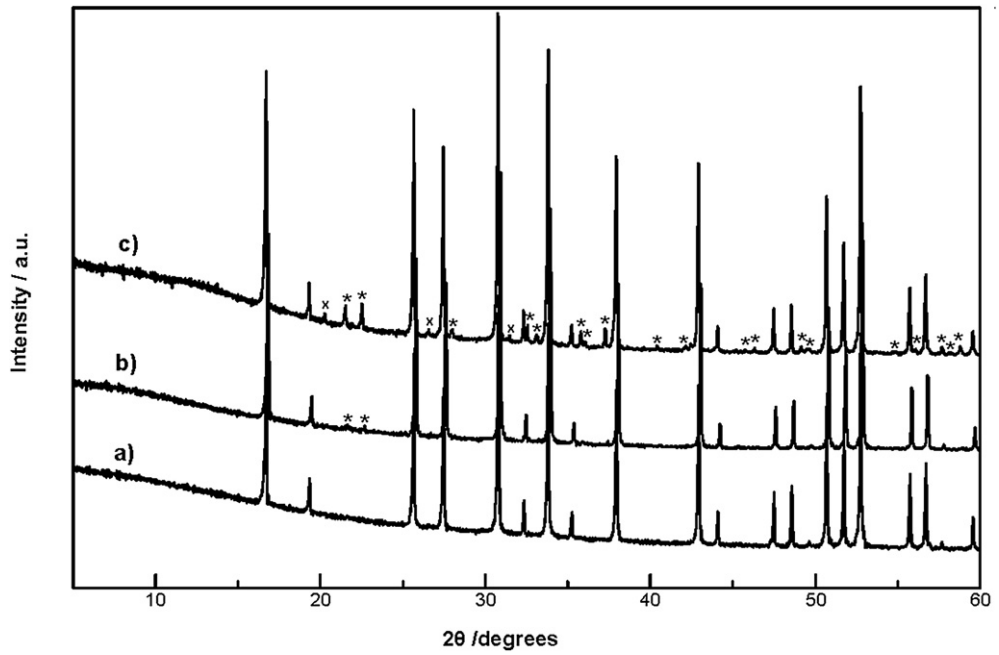

Fig. 3. XRD patterns of (a) 0.4Ga-LLZO, (b) 0.5Ga-LLZO and (c) 1.0Ga-LLZO samples. Kα_2 contribution was eliminated, using Rachinger method, for clarification. (*): $LiGaO_2$ (ICSD, PDF-00-023-0359); (x): Li_2ZrO_3 (ICSD, PDF-00-033-0843).

real *Z* axis. These intercepts, hence, correspond to the total resistance of the material. This suggests that the "low frequency" semicircle observed for our materials would correspond to electrode effects. The total conductivity for different gallium-containing samples was therefore estimated from the fitting data of the "high frequency" semicircle. And for the 1.0Ga-LLZO sample, the intercept (at the high frequency side) with the real *Z* axis was taken as the total resistance.

The measured conductivities of one batch of the samples at 20 °C are 3.8×10^{-5}, 4.4×10^{-5}, 8.9×10^{-5} and 5.4×10^{-4} S cm^{-1} for 0.3Ga-LLZO, 0.4Ga-LLZO, 0.5Ga-LLZO and 1.0Ga-LLZO samples, respectively. The conductivity clearly increases with increasing the

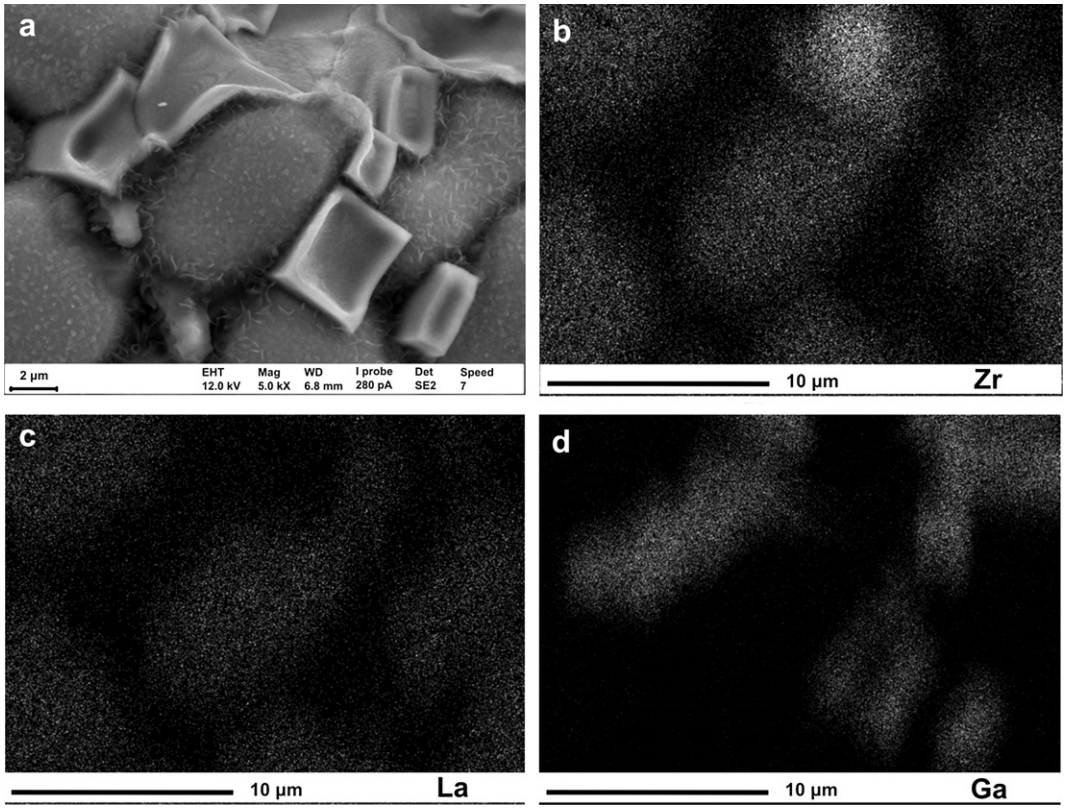

Fig. 4. SEM image of 1.0Ga-LLZO (a), and corresponding EDX mapping of Zr (b), La (c) and Ga (d).

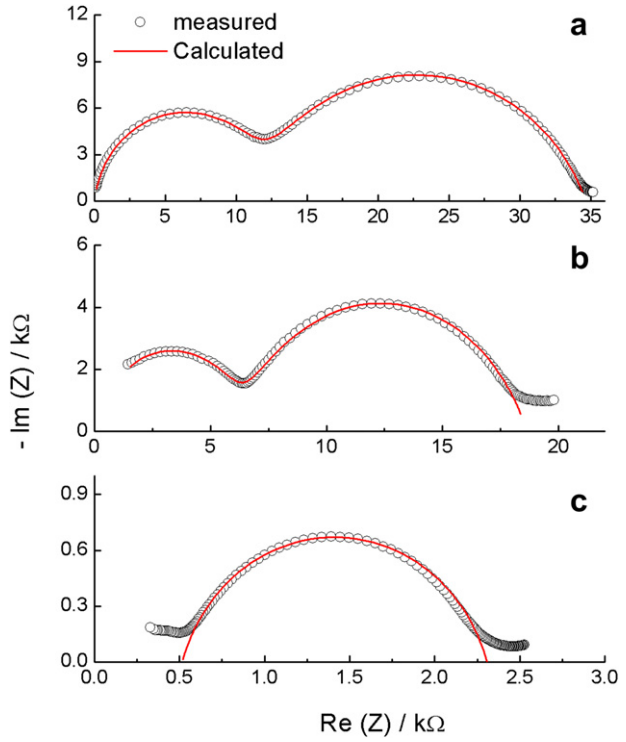

Fig. 5. Typical impedance plots for (a) 0.4Ga-LLZO, (b) 0.5Ga-LLZO and (c) 1.0Ga-LLZO samples, using Li electrodes (frequency range from 7 MHz to 1 Hz, at 20 mV amplitude) at room temperature. Data were fitted using the equivalent circuits (RQ)(RQ) or (R)(RQ).

gallium content. A second pellet, with different geometry, of 1.0Ga-LLZO has shown the conductivities 4.5×10^{-4} and 4.3×10^{-4} S cm^{-1} using Au and Li electrodes, respectively, at room temperature (~22 °C). The average conductivity observed for the 1.0Ga-LLZO sample is comparable to that reported by Muruganet al. [1]. However, it should be noted that the material is free of aluminium and is fully stabilized by gallium. The stabilization is also achieved in a quantitative manner at significantly reduced sintering time and temperature. Density of 1.0Ga-LLZO is 92.5% of the theoretical density, which is comparable to that reported by Murugan et al. (92%) [1]. The material is also stable in contact with lithium metal.

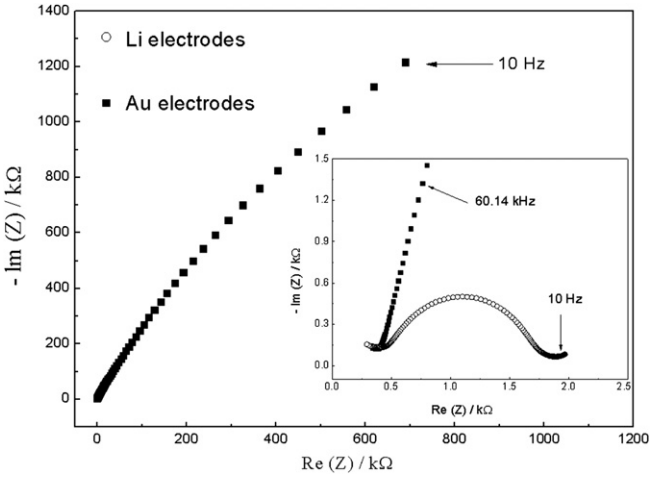

Fig. 6. Impedance spectra for the 1.0Ga-LLZO sample measured using Li electrodes and Au electrodes, respectively, under inert atmosphere. The inset shows a zoom in order to magnify the plot corresponding to Li electrodes.

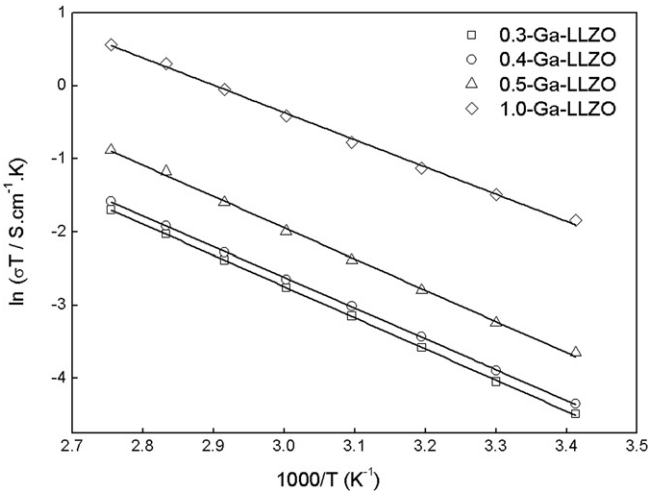

Fig. 7. Arrhenius plots for the electrical conductivity of different gallium-containing LLZO samples.

No change in colour or composition (as indicated by XRD) is observed for a 1.0Ga-LLZO pellet kept under contact with metallic lithium for more than one month at room temperature.

The variation of conductivity with temperature was studied in the temperature range 20–90 °C. Arrhenius plots of the total electrical conductivity of different gallium-containing LLZO phases are shown in Fig. 7. The observed activation energies for the conductivity of the 0.3Ga-LLZO, 0.4Ga-LLZO, 0.5Ga-LLZO and 1.0Ga-LLZO samples are 0.37, 0.36, 0.36 and 0.32 eV, respectively. No sign of interaction between lithium metal and the samples was observed in the studied temperature range. The activation energy for the total conductivity of the 1.0Ga-LLZO sample lies in the same range that was observed for cubic LLZO phases [1]; however, the activation energies observed for the samples containing less gallium are slightly higher, probably due to insufficient sintering and increasing the grain-boundary resistance. This would also provide a confirmation that the measured conductivities include the grain-boundary effects.

Hence, incorporation of gallium in LLZO phases leads to stabilization of cubic garnet phases with fast ion-conducting properties. Conductivity is improved by increasing the gallium content where gallium ions, in the form of $LiGaO_2$, act as a sintering aid and result in more dense material. Densification reduces the grain-boundary resistance and enhances the lithium ion conductivity. Despite the fact that lithium ion conductivity of $LiGaO_2$ is fairly low [20,21], the material, which is resided at the grain boundaries, would in part support lithium ion transport between the grains by filling voids between them. This will minimize the grain-boundary resistance and probably account for the good transport properties observed for these materials. Similar effect has been observed for LLZO phases containing Al/Si [9]. Al^{3+} and Si^{4+} ions were incorporated in these materials by the materials used for ball milling and crucibles. Amorphous Li–Al–Si–O with nano-crystalline $LiAlSiO_4$ presented at the grain boundaries of these materials was assumed to minimize the grain-boundary resistance.

4. Conclusions

Lithium-stuffed garnets of the LLZO type, with cubic structure and fast lithium ion conductivity (up to $\sim 5 \times 10^{-4}$ S cm^{-1}), have been stabilized by gallium addition. This new approach of stabilizing cubic HT-LLZO phases provides materials with good sinterability at relatively low sintering time and temperature (1085 °C/6 h). The

approach also provides a quantitative and reproducible route of synthesis, which reduces the difficulties associated with preparing these materials. Under the applied synthesis condition, gallium ions clearly stabilize the cubic garnet phase at gallium content $\geq$0.3 moles per mole of LLZO. The garnet structure was stable up to 1.0 mole addition of gallium. Excess gallium ions combine with excess lithium ions to form $LiGaO_2$ which acts as a sintering aid and significantly improves lithium ion conductivity. $LiGaO_2$ is resided at the grain boundaries giving rise to possible routes for lithium ion transport between the grains.

Acknowledgements

We like to thank the Alexander von Humboldt foundation for a postdoc grant and financial support (Dr. Hany El Shinawi). We are also grateful to Dr. Klaus Peppler for assistance with SEM and EDX measurements.

Appendix A. Supplementary data

Supplementary data related to this article can be found at doi:10.1016/j.jpowsour.2012.09.111.

References

[1] R. Murugan, V. Thangadurai, W. Weppner, Angew. Chem. Int. Ed. 46 (2007) 7778–7781.
[2] M. Kotobuki, H. Munakata, K. Kanamura, Y. Sato, T. Yoshida, J. Electrochem. Soc. 157 (2010) A1076–A1079.
[3] J. Awaka, N. Kijima, H. Hayakawa, J. Akimoto, J. Solid State Chem. 182 (2009) 2046–2052.
[4] Y. Shimonishi, A. Toda, T. Zhang, A. Hirano, N. Imanishi, O. Yamamoto, Y. Takeda, Solid State Ionics 183 (2011) 48–53.
[5] I. Kokal, M. Somer, P.H.L. Notten, H.T. Hintzen, Solid State Ionics 185 (2011) 42–46.
[6] H. Xie, J.A. Alonso, Y. Li, M.T. Fernandez-Díaz, J.B. Goodenough, Chem. Mater. 23 (2011) 3587–3589.
[7] C.A. Geiger, E. Alekseev, B. Lazic, M. Fisch, T. Armbruster, R. Langner, M. Fechtelkord, N. Kim, T. Pettke, W. Weppner, Inorg. Chem. 50 (2011) 1089–1097.
[8] H. Buschmann, J. Dölle, S. Berendts, A. Kuhn, P. Bottke, M. Wilkening, P. Heitjans, A. Senyshyn, H. Ehrenberg, A. Lotnyk, V. Duppel, L. Kienle, J. Janek, Phys. Chem. Chem. Phys. 13 (2011) 19378–19392.
[9] S. Kumazakia, Y. Iriyamaa, K. Kimb, R. Murugan, K. Tanabeb, K. Yamamotob, T. Hirayamab, Z. Ogumi, Electrochem. Commun. 13 (2011) 509–512.
[10] M. Kotobuki, K. Kanamura, Y. Sato, T. Yoshida, J. Power Sources 196 (2011) 7750–7754.
[11] E. Rangasamy, J. Wolfenstine, J. Sakamoto, Solid State Ionics 206 (2012) 28–32.
[12] R. Murugan, S. Ramakumar, N. Janani, Electrochem. Commun. 13 (2011) 1373–1375.
[13] A.C. Larson, R.B. Von Dreele, General Structural Analysis System, Los Alamos National Laboratory, Los Alamos, NM, 1994.
[14] J.T.S. Irvine, D.C. Sinclair, A.R. West, Adv. Mater. 2 (1990) 132–138.
[15] E. Quartarone, P. Mustarelli, Chem. Soc. Rev. 40 (2011) 2525–2540.
[16] V. Thangadurai, H. Kaack, W. Weppner, J. Am. Ceram. Soc. 86 (2003) 437–440.
[17] V. Thangadurai, W. Weppner, J. Am. Ceram. Soc. 88 (2005) 411–418.
[18] V. Thangadurai, W. Weppner, Adv. Funct. Mater. 15 (2005) 107–112.
[19] S. Narayanan, V. Thangadurai, J. Power Sources 196 (2011) 8085–8090.
[20] R.J. Grant, I.M. Hodge, M.D. Ingram, A.R. West, J. Am. Ceram. Soc. 60 (1977) 226.
[21] P. Quintana, F. Velasco, A.R. West, Solid State Ionics 34 (1989) 149–155.